

# Luminescence of nanocrystalline ZnSe:Mn<sup>2+</sup>

J. F. Suyver,\* S. F. Wuister, J. J. Kelly and A. Meijerink

Debye Institute, Physics and Chemistry of Condensed Matter, Utrecht University,  
P.O. Box 80.000, 3508 TA Utrecht, The Netherlands. E-mail: j.f.suyver@phys.uu.nl;  
Fax: +31-30-253 2403; Tel: +31-30-253 2241

Received 25th August 2000, Accepted 12th October 2000

First published as an Advance Article on the web 9th November 2000

The luminescence properties of nanocrystalline ZnSe:Mn<sup>2+</sup> prepared *via* an inorganic chemical synthesis are described. Photoluminescence spectra show distinct ZnSe and Mn<sup>2+</sup> related emissions, both of which are excited *via* the ZnSe host lattice. The Mn<sup>2+</sup> emission wavelength and the associated luminescence decay time depend on the concentration of Mn<sup>2+</sup> incorporated in the ZnSe lattice. Temperature-dependent photoluminescence spectra and photoluminescence lifetime measurements are also presented and the results are compared with those of Mn<sup>2+</sup> in bulk ZnSe.

## 1 Introduction

Quantum size effects in nanocrystalline semiconductors such as CdS, CdSe, ZnS and ZnO have been studied extensively.<sup>1–6</sup> In some cases the method for synthesis of nm semiconductor particles is a simple room temperature reaction in water or alcohol (*e.g.* CdS, ZnS or ZnO).<sup>4–6</sup> In other cases, more elaborate and challenging high temperature reactions with air and moisture-sensitive reactants are applied to obtain highly efficient luminescing nanocrystals (*e.g.* CdSe).<sup>1,2</sup> In addition to undoped semiconductor nanocrystals, the luminescence of nanocrystalline semiconductors in which optically active ions are incorporated has received considerable attention, also in relation to possible applications.<sup>1,2</sup> A simple wet chemical synthesis is attractive for device applications since large amounts of well-defined nanocrystals (NC) can easily be obtained in this way. As a result, many studies have focused on ZnS and CdS doped with Mn<sup>2+</sup> or trivalent lanthanides.<sup>5</sup>

Efficiently luminescing ZnS:Mn<sup>2+</sup> nanocrystals [quantum efficiency (QE) of more than 10%] can easily be made and are considered for application in low voltage electroluminescent devices.<sup>7,8</sup> However, the position of the ZnS valence band-edge is located too far from the vacuum-level for direct injection of holes from presently available *p*-type conducting polymers. Better results are expected for ZnSe which has a valence band-edge at higher energy with respect to ZnS.<sup>9</sup>

To date, there have been no reports (as far as the authors are aware) on the synthesis and luminescence properties of nanocrystalline ZnSe doped with a luminescent ion, such as Mn<sup>2+</sup>. This is probably because the synthesis of nanocrystalline ZnSe particles is not as simple as that of ZnS particles. Undoped ZnSe particles with quantum efficiencies of 1–5% can be obtained by a high temperature (300 °C) synthesis in the organic soap hexadecylamine.<sup>10</sup>

In this paper the preparation of nanocrystalline ZnSe particles doped with Mn<sup>2+</sup> is discussed. It will be shown that Mn<sup>2+</sup> can be incorporated in nanocrystalline ZnSe. Photoluminescence (PL) emission and excitation spectra are presented and discussed. Temperature-dependent luminescence and luminescence lifetime measurements are also reported and compared with results obtained for the luminescence of Mn<sup>2+</sup> in bulk ZnSe.

## 2 Experimental

The synthesis route that was used to prepare the ZnSe:Mn<sup>2+</sup> nanocrystals is a variation of the trioctylphosphine/trioctyl-

phosphine oxide (TOP/TOPO) synthesis (used for CdSe)<sup>11</sup> which yields ZnSe nanocrystals with quantum efficiencies of 1–5%.<sup>10</sup> The synthesis was performed in the protective dry-nitrogen atmosphere of a glovebox. Hexadecylamine (HDA) was used as the solvent instead of TOPO because its bond to Zn is weaker and it is less alkaline than TOPO.<sup>10</sup> A 45 ml sample of HDA was heated to 310 °C in a flask. A variable amount of manganese cyclohexanecarboxylate powder was dissolved in 12 ml of TOP for samples with different Mn<sup>2+</sup> concentrations. To this mixture 3 ml of a 1 M solution of TOPSe (previously prepared by dissolving elemental Se powder in TOP) were added. After stirring, 0.32 g of di-ethylzinc was added. This solution was shaken and then added to the hot HDA using a syringe. The nanocrystals were grown at 275 °C for 4 h. The mixture was then cooled to 70 °C and the nanocrystals were precipitated by addition of 25 ml of anhydrous butan-1-ol followed by 30 ml of anhydrous methanol. The residue was taken out of the glovebox, centrifuged and decanted. The samples were returned to the glovebox and washed with anhydrous methanol. Finally, the samples were dried in a vacuum desiccator, and a fine white powder was obtained. This powder consists of the ZnSe:Mn<sup>2+</sup> nanocrystals with a HDA capping.

The chemical composition of the samples was determined using a Perkin-Elmer Optima-3000 inductively coupled plasma (ICP) spectrometer. To determine the particle diameter, X-ray powder diffraction spectra were measured with a Philips PW 1729 X-ray diffractometer using Cu K $\alpha$  radiation ( $\lambda = 1.542 \text{ \AA}$ ). The X-ray diffraction (XRD) spectrum showed broad peaks at positions that are in good agreement with the zincblende modification of ZnSe.<sup>12</sup> The broadening of the XRD lines is attributed to the nanocrystalline nature of the samples and was used to calculate the diameter of the nanocrystals by means of the Debye–Scherrer equation.<sup>13</sup>

Photoluminescence (PL) emission and excitation spectra were recorded with a SPEX Fluorolog spectrofluorimeter, Model F2002, equipped with two monochromators (double-grating, 0.22 m, SPEX 1680) and a 450 W xenon lamp as the excitation source. All photoluminescence emission spectra were corrected for the spectral response of the emission monochromator and the photomultiplier tube. PL lifetimes were measured using the third harmonic (355 nm) of a Quanta-ray DCR Nd:YAG laser as an excitation source. The emission light was transported through a fibre optic cable to a monochromator (Acton SP-300i, 0.3 m, 150 lines mm<sup>-1</sup> grating, blazed at 500 nm). The signals were recorded using a ther-

moelectrically cooled photomultiplier tube in combination with a Tektronix 2430 oscilloscope. Temperature-dependent PL emission and lifetime spectra were recorded using a liquid helium flow-cryostat equipped with a sample heater to stabilize the temperature at different temperatures between 4 K and room temperature.

### 3 Results and discussion

The amounts of Mn, Zn and Se present in the ZnSe:Mn<sup>2+</sup> samples were measured using ICP analysis. Typically, 10% of the initial Mn<sup>2+</sup> that was present during the synthesis was incorporated in the ZnSe lattice. The highest Mn<sup>2+</sup> concentration in the ZnSe nanocrystals was found to be 3%. However, the yield of material resulting from the syntheses with [Mn<sup>2+</sup>] > 1% incorporated was very low. This low yield may be due to the organic residue from the Mn<sup>2+</sup> precursor which can hinder the formation of the ZnSe nanocrystals. Only samples with [Mn<sup>2+</sup>] < 1% were used in the measurements that are discussed below. X-ray powder diffraction analysis indicated that the particles had a radius *r* in the range 3–4 nm, and no relation between size and the Mn<sup>2+</sup> concentration was observed.

#### 3.1 PL excitation and emission

Fig. 1 shows the photoluminescence emission spectra of several nanocrystalline ZnSe:Mn<sup>2+</sup> samples with [Mn<sup>2+</sup>] between 0 and 0.9%. The measurement conditions were identical in all cases and therefore relative intensities can be compared. The photoluminescence peak around 430 nm is attributed to a sub-bandgap luminescence of the ZnSe host lattice. The peak at ~560 nm is attributed to the <sup>4</sup>T<sub>1</sub> → <sup>6</sup>A<sub>1</sub> transition in the Mn<sup>2+</sup> ion. The position of the Mn<sup>2+</sup> emission is similar to that for Mn<sup>2+</sup> in bulk ZnSe.<sup>14,15</sup> On the lower energy side (600–640 nm) a third emission band is usually found for bulk ZnSe:Mn<sup>2+</sup>. This band is assigned to a self-activated (SA) luminescence, probably due to Cl<sub>S</sub><sup>-</sup>-V<sub>Zn</sub><sup>''</sup> donor-acceptor pairs. (Here the Kröger-Vink notation is used for identifying defects.<sup>16</sup>) The observation that this SA luminescence is absent (or very weak) indicates that the concentration of Cl<sub>S</sub><sup>-</sup>-V<sub>Zn</sub><sup>''</sup> pairs in the ZnSe nanocrystals is low. This may be due to the small size (low probability for the presence of both types of defect in one nanocrystal) and to the purity of the chemicals used in the synthesis.

The total luminescence quantum efficiency (QE) for each sample (indicated in Fig. 1) shows a large decrease in the ZnSe related emission with increasing [Mn<sup>2+</sup>] even for low incorp-

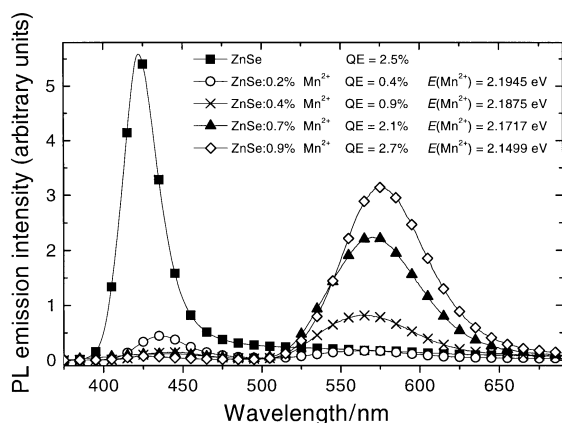


**Fig. 1** Photoluminescence emission spectra for nanocrystalline ZnSe:Mn<sup>2+</sup> samples with different Mn<sup>2+</sup> concentrations, as indicated in the figure. All spectra were measured at room temperature and the excitation wavelength was 330 nm. The symbols (squares, circles, crosses and triangles) are used to label the different spectra and the drawn lines are the measured spectra. This is the case for all figures in this paper.

orated Mn<sup>2+</sup> concentrations. It is known from the literature that efficient energy transfer from the ZnSe host-lattice to the Mn<sup>2+</sup> dopant is possible.<sup>17</sup> However, the decrease of the ZnSe related emission is not only due to energy transfer to Mn<sup>2+</sup>. The drop in the overall QE from 2.5 to 0.4% for the incorporation of 0.2% Mn<sup>2+</sup> indicates that non-radiative quenching centres are also introduced in the synthesis including the Mn<sup>2+</sup> precursor. This is believed to be caused by the organic residue from the Mn<sup>2+</sup> precursor, which may induce defects in the NC, or result in efficient quenching states on its surface.

At higher Mn<sup>2+</sup> concentrations, the energy transfer to Mn<sup>2+</sup> becomes more efficient and the intensity of the yellow Mn<sup>2+</sup> emission increases. For 0.9% Mn<sup>2+</sup> the QE has increased to 2.7%, just above that of the ZnSe related emission in the undoped sample. The present results are typical for one concentration series of Mn<sup>2+</sup> doped ZnSe nanocrystals. Since the quantum efficiencies of doped and undoped nanocrystalline semiconductors are strongly dependent on small variations in the synthesis procedure, higher quantum efficiencies can be expected on optimizing the synthesis procedure. Better results may also be obtained with another type of Mn<sup>2+</sup> precursor. These points require further investigation.

The observed PL emission energies for Mn<sup>2+</sup>, obtained from a Gaussian fit of the Mn<sup>2+</sup> related PL peak, are given in Fig. 1. A shift in the maximum of the Mn<sup>2+</sup> emission to lower energy is observed for increasing Mn<sup>2+</sup> concentrations. This shift is possibly due to the formation of pairs of Mn<sup>2+</sup> ions at higher concentrations. It is well known that the emission of Mn<sup>2+</sup> pairs can be at lower energy than that of single ions.<sup>18</sup> Lifetime measurements presented below provide additional evidence for the formation of Mn<sup>2+</sup> pairs at higher Mn<sup>2+</sup> concentrations.

Photoluminescence excitation spectra of both the ZnSe and the Mn<sup>2+</sup> related emission show a clear maximum for excitation at ~370 nm, as is shown in Fig. 2, where  $\phi$  denotes the photon flux per constant wavelength interval. The steep increase beyond 390 nm in the excitation spectrum for the ZnSe related emission is due to the detection of scattered excitation light which is not rejected by the monochromator, since the wavelength of the emission monochromator ( $\lambda = 418$  nm) is close to the excitation wavelength. The position of the excitation maximum was found to vary slightly from sample to sample; a small variation in particle size (and thus in the bandgap) can explain such differences. The particle radius could not be calculated using the Brus equation<sup>3</sup> because the values of the electron and hole effective masses are not known in ZnSe.

The fact that both ZnSe and Mn<sup>2+</sup> have the same excitation maximum indicates that the excitation of the divalent manganese takes place through energy transfer from the ZnSe

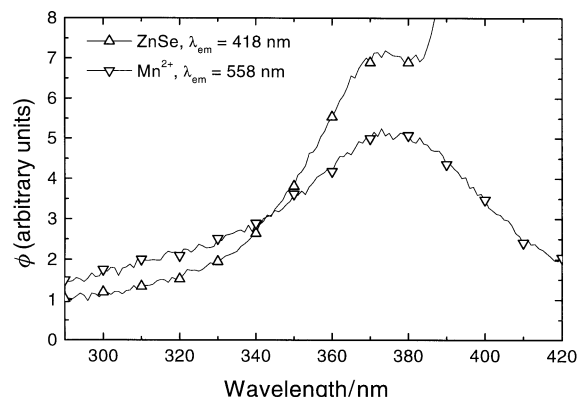


**Fig. 2** Photoluminescence excitation spectra for the ZnSe:0.2% Mn<sup>2+</sup> sample. The spectra were measured at room temperature and the emission wavelengths are indicated in the figure. The values of  $\phi$  for the two curves cannot be compared.

host lattice. This agrees with the observation based on Fig. 1 that incorporation of  $\text{Mn}^{2+}$  in the ZnSe lattice results in a decrease of the ZnSe related PL and a concomitant increase in the  $\text{Mn}^{2+}$  PL. Efficient energy transfer to  $\text{Mn}^{2+}$  centres incorporated in ZnSe has been well studied in bulk ZnSe: $\text{Mn}^{2+}$  (ref. 19) and the same efficient transfer is expected to occur in nanocrystalline ZnSe: $\text{Mn}^{2+}$ , as is indeed observed.

### 3.2 Luminescence lifetime

The time dependence of the ZnSe and  $\text{Mn}^{2+}$  luminescence intensity after pulsed excitation was measured for all the samples referred to in Fig. 1. The ZnSe luminescence ( $\lambda = 440$  nm) decay curves were found to have  $\sim 100$  ns components as well as components that were too fast to be measured with the experimental set-up used. Fig. 3 shows the  $\text{Mn}^{2+}$  luminescence ( $\lambda = 550$  nm) decay curves for all the samples, measured at room temperature and scaled at  $t = 0$ . Four single-exponential fits of the spectrum up to 1 ms are shown as lines through the data. In all cases a lifetime of the order of 200  $\mu\text{s}$  was found. The exact values of the lifetimes are indicated in the figure. Even though the fits shown in Fig. 3 describe the experimental data fairly well, the decay is not purely single exponential and, depending on the time interval used in the fitting procedure, different lifetimes are found. When the  $\text{Mn}^{2+}$  related emission beyond 1 ms is fitted, even a weak ms component to the  $\text{Mn}^{2+}$  lifetime could be identified. The samples containing more  $\text{Mn}^{2+}$  have shorter lifetimes and a drop from  $\sim 290$  to  $\sim 190$   $\mu\text{s}$  is observed between 0.2 and 0.9%  $\text{Mn}^{2+}$ . Finally, a fast ( $\sim 100$  ns) component is also observed, which is assigned to ZnSe related emission, by analogy with results for ZnS: $\text{Mn}^{2+}$ .<sup>20,21</sup>

The interpretation of the measured lifetimes and the concentration dependence is not straightforward. In spite of extensive research on bulk ZnSe: $\text{Mn}^{2+}$ , the radiative lifetime of the  $\text{Mn}^{2+}$  emission (from single ions) is not well established; values between 30 and 800  $\mu\text{s}$  have been reported.<sup>14,15,22</sup> At room temperature the lifetime is reduced by thermal quenching, which has been found to be sample-dependent. The concentration also influences the lifetime; even at  $\text{Mn}^{2+}$  concentrations as low as 1% a reduction in the lifetime has been reported.<sup>15</sup> Owing to the uncertainty in the single ion radiative lifetime and the non-exponential character of the luminescence decay curve, it is difficult to derive quantitative information from the luminescence decay results of Fig. 3. However, two qualitative conclusions can be made.

Firstly, the lifetime of the  $\text{Mn}^{2+}$  emission in ZnSe is of the order of hundreds of  $\mu\text{s}$ , *i.e.* shorter than for  $\text{Mn}^{2+}$  in ZnS ( $\tau = 1.8$  ms). This has been observed before and is explained by stronger spin-orbit coupling due to the heavier  $\text{Se}^{2-}$  ligands in comparison with  $\text{S}^{2-}$ .<sup>22</sup>

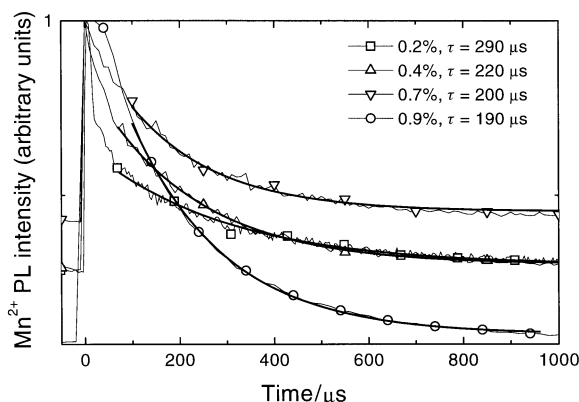


Fig. 3 Decay curves of the  $\text{Mn}^{2+}$  related emission at room temperature for different  $\text{Mn}^{2+}$  concentrations in ZnSe. The pulsed excitation wave length was 355 nm.

Secondly, the lifetime of the emission is shorter at higher  $\text{Mn}^{2+}$  concentrations ( $\sim 290$   $\mu\text{s}$  at 0.2%  $\text{Mn}^{2+}$  and  $\sim 190$   $\mu\text{s}$  at 0.9%  $\text{Mn}^{2+}$ ). The concentration range in which a shortening of the lifetime is observed is too low to be explained by random pair formation. It is however known that due to exchange interaction the spin selection rule is partially lifted and the lifetime of the  $\text{Mn}^{2+}$  emission is reduced at higher concentrations when exchange-coupled  $\text{Mn}^{2+}$  pairs are formed.

In combination with previous evidence for pair-formation (the shift of the  $\text{Mn}^{2+}$  emission to longer wavelengths with increasing  $\text{Mn}^{2+}$  concentration) the shorter lifetimes at higher concentrations may well be due to exchange-coupled  $\text{Mn}^{2+}$  pairs. The relatively important contribution of  $\text{Mn}^{2+}$  pairs at low  $\text{Mn}^{2+}$  concentration might be due to preferential pair formation or to faster trapping of electron-hole pairs after bandgap excitation by the  $\text{Mn}^{2+}$  pair-states. Both suggestions have been made previously for bulk ZnSe: $\text{Mn}^{2+}$ .<sup>23</sup>

### 3.3 Temperature dependence

Fig. 4 shows temperature-dependent measurements of the photoluminescence spectra for a ZnSe: $\text{Mn}^{2+}$  sample. The quenching of the ZnSe and  $\text{Mn}^{2+}$  related PL intensities has also been reported for bulk ZnSe: $\text{Mn}^{2+}$  (ref. 22 and 24) and were explained in ref. 25.

A clear shift of the ZnSe related PL emission energy to longer wavelengths is also observed for increasing temperature in Fig. 4. This shift could be fitted very well using a standard equation for the temperature dependence of the bandgap<sup>26</sup>

$$E_g(T) = E_0 - \frac{\alpha T^2}{T + \beta}, \quad (1)$$

where  $E_0$  represents the bandgap at 0 K and  $\alpha$  and  $\beta$  are fitting parameters. It is known from the literature that  $\beta$  is of the order of the Debye temperature of the semiconductor ( $\theta_D$ ). This equation takes into account both the change in lattice parameter and the temperature dependence of the electron-lattice interaction. It should be noted that eqn. (1) was originally derived for the infinite crystal approximation and has (as far as the authors are aware) only been used to analyse bulk semiconductor systems. It is not immediately obvious that this equation will also apply to nanocrystalline materials which have a different band-structure and a different phonon density of states.

The temperature dependence of the ZnSe related PL could be fitted with eqn. (1), as is shown in Fig. 5(a). From these fits, values of  $\alpha = (9 \pm 3) \times 10^{-4}$  eV  $\text{K}^{-1}$  and  $\beta = (3.8 \pm 0.5) \times 10^2$  K were found. The value of  $\alpha$  compares well with that found for bulk ZnSe ( $7.5 \times 10^{-4}$  eV  $\text{K}^{-1}$ ) and the value of  $\beta$  is slightly larger than that reported for bulk ZnSe (295 K).<sup>27</sup> The larger value of  $\beta$  might be explained by noting that  $\beta$  is a

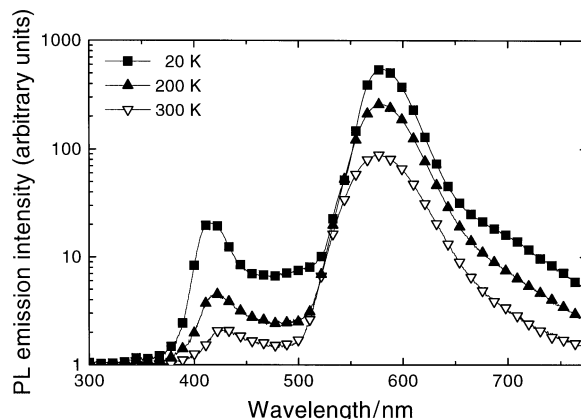


Fig. 4 Temperature-dependent PL spectra for the ZnSe:0.7%  $\text{Mn}^{2+}$  sample. Note the logarithmic intensity axes. Excitation was at 330 nm.

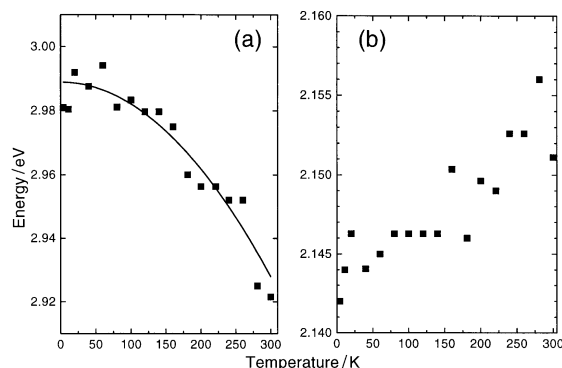
measure of the Debye temperature of the semiconductor (for bulk ZnSe  $\theta_D = 400$  K<sup>28</sup>) and that the Debye temperature of a nanocrystal is expected to be slightly higher than the bulk value due to phonon cut-off at low energy as a result of the small dimensions of the crystal.

Fig. 5(b) shows the change in  $\text{Mn}^{2+}$  related photoluminescence emission energy as a function of temperature. The shift of the  $\text{Mn}^{2+}$  emission energy to shorter wavelength has also been observed in bulk ZnSe: $\text{Mn}^{2+}$ .<sup>25</sup> However, the measured blue-shift between 4 and 300 K for nanocrystalline ZnSe: $\text{Mn}^{2+}$  of  $(15 \pm 2)$  meV is slightly less than in the bulk system (23 meV), which might be due to a slightly different lattice expansion for a ZnSe nanocrystal compared with bulk ZnSe.

Fig. 6 shows the temperature dependence of the  $\text{Mn}^{2+}$  related PL lifetime for a ZnSe:0.2%  $\text{Mn}^{2+}$  sample. In contrast to previous results for ZnS: $\text{Mn}^{2+}$ , a temperature quenching of the lifetime is observed. When the temperature-induced quenching of the  $\text{Mn}^{2+}$  lifetime is fitted on the basis of a simple temperature-activated process, an energy  $\Delta E = 22.3$  meV is found, regardless of the  $\text{Mn}^{2+}$  concentration present in the ZnSe lattice. The decrease in lifetime can be explained by thermally activated energy transfer to quenching centres since in the same temperature regime where the luminescence lifetime becomes shorter, the luminescence intensity decreases.

## 4 Conclusions

This paper presents a chemical synthesis method to prepare powders of ZnSe nanocrystals ( $r \sim 3\text{--}4$  nm) doped with  $\text{Mn}^{2+}$ . The photoluminescence emission spectra of these samples show a ZnSe related near-band-edge emission at  $\sim 440$  nm and a  $\text{Mn}^{2+}$  related band at  $\sim 560$  nm. The wavelength of the  $\text{Mn}^{2+}$  related emission shifts to lower energy for



**Fig. 5** Spectra for the ZnSe:0.9%  $\text{Mn}^{2+}$  sample. (a) Temperature dependence of the ZnSe related emission energy. The line through the data is a fit of eqn. (1). (b) Maximum energy of the  $\text{Mn}^{2+}$  related photoluminescence as a function of the temperature.

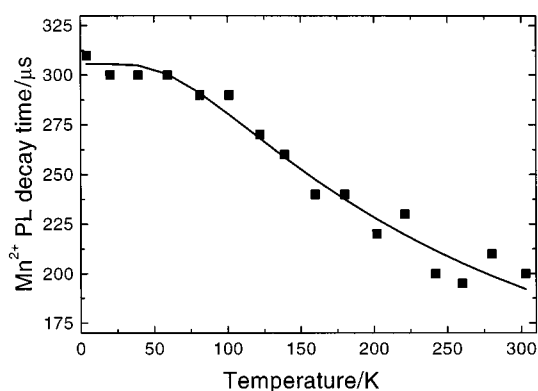


**Fig. 6** Temperature-dependent lifetimes of the  $\text{Mn}^{2+}$  PL for a ZnSe:0.2%  $\text{Mn}^{2+}$  sample. Pulsed excitation at 355 nm was used. The line is a fit to the data for a temperature-activated process.

increasing amounts of  $\text{Mn}^{2+}$  incorporated in the ZnSe lattice. The photoluminescence excitation spectrum shows that the divalent manganese can be excited through the ZnSe host lattice.

The  $\text{Mn}^{2+}$  luminescence decay curves show a lifetime of  $\sim 290$   $\mu\text{s}$ , which decreases with increasing  $[\text{Mn}^{2+}]$ . This decrease in lifetime may be due to the formation of  $\text{Mn}^{2+}$  pairs in the nanocrystal. The temperature dependence of the  $\text{Mn}^{2+}$  lifetime can be explained by a temperature-activated quenching with an activation energy of 22.3 meV. The ZnSe related luminescence has a temperature-induced shift similar to that of bulk ZnSe. The self-activated emission ( $\lambda \sim 640$  nm), often observed in bulk ZnSe: $\text{Mn}^{2+}$ , is not present in these nanocrystals.

## 5 Acknowledgements

Marieke van Veen is acknowledged for valuable discussions. This work is part of the Research Program of the Priority Program for new Materials (PPM) and was made possible by financial support from the Dutch Association for Scientific Research (NWO).

## References

- 1 N. C. Greenham, X. Peng and A. P. Alivisatos, *Phys. Rev. B*, 1996, **54**, 17628.
- 2 B. O. Dabbousi, M. G. Bawendi, O. Onitsuka and M. F. Rubner, *Appl. Phys. Lett.*, 1995, **66**, 1316.
- 3 L. Brus, *J. Phys. Chem.*, 1986, **90**, 2555.
- 4 R. N. Bhargava, D. Gallagher, X. Hong and A. Nurmikko, *Phys. Rev. Lett.*, 1994, **72**, 416.
- 5 I. Yu, T. Isobe and M. Senna, *J. Phys. Chem. Solids*, 1996, **57**, 373.
- 6 A. van Dijken, E. A. Meulenkaamp, D. Vanmaekelbergh and A. Meijerink, *J. Phys. Chem. B*, 2000, **104**, 1715.
- 7 J. Leeb, V. Gebhardt, G. Müller, D. Su, M. Giersig, G. McMahon and L. Spanhel, *J. Phys. Chem. B*, 1999, **103**, 7839.
- 8 J. F. Suyver, R. Bakker, A. Meijerink and J. J. Kelly, *Phys. Status Solidi A*, 2001, in the press.
- 9 G. H. Schoenmakers, E. P. A. M. Bakkers and J. J. Kelly, *J. Electrochem. Soc.*, 1997, **144**, 2329.
- 10 M. A. Hines and P. Guyot-Sionnest, *J. Phys. Chem. B*, 1998, **108**, 3655.
- 11 C. B. Murray, D. J. Norris and M. G. Bawendi, *J. Am. Chem. Soc.*, 1993, **115**, 8706.
- 12 R. Jenkins, W. F. McClune, T. M. Maguire, M. A. Holomany, M. E. Mrose, B. Post, S. Weissmann, H. F. McMurdie and L. Zwell, *Powder Diffraction File*, JCPDS International Center for Diffraction Data, 1985.
- 13 B. D. Cullity, *Elements of X-ray Diffraction*, Addison Wesley, Reading, MA, 1978, p. 102.
- 14 H. Waldmann, C. Benecke, W. Busse, H.-E. Gumlich and A. Krost, *Semicond. Sci. Technol.*, 1989, **4**, 71.
- 15 D. F. Crabtree, *Phys. Status Solidi A*, 1974, **22**, 543.
- 16 F. A. Kröger, *The Chemistry of Imperfect Crystals*, North-Holland, Amsterdam, 1973.
- 17 N. E. Rigby and J. W. Allen, *J. Lumin.*, 1988, **42**, 143.
- 18 C. R. Ronda and T. Amrein, *J. Lumin.*, 1996, **69**, 245.
- 19 U. Stutenbäumer, H.-E. Gumlich and H. Zuber, *Phys. Status Solidi B*, 1989, **156**, 561.
- 20 N. Murase, R. Jagannathan, Y. Kanematsu, M. Watanabe, A. Kurita, K. Hirata, T. Yazawa and T. Kushida, *J. Phys. Chem. B*, 1999, **103**, 754.
- 21 A. A. Bol and A. Meijerink, *Phys. Rev. B*, 1998, **58**, 15997.
- 22 T. C. Leslie and J. W. Allen, *Phys. Status Solidi A*, 1981, **65**, 545.
- 23 S. J. Weston, M. O'Neill, J. E. Nicholls, J. Miao, W. E. Hagston and T. Stirner, *Phys. Rev. B*, 1998, **58**, 7040.
- 24 J. F. MacKay, W. M. Becker, J. Spałec and U. Debska, *Phys. Rev. B*, 1990, **42**, 1743.
- 25 J. Xue, Y. Ye, F. Medina, L. Martinez, S. A. Lopez-Rivera and W. Giriat, *J. Lumin.*, 1998, **78**, 173.
- 26 Y. P. Varshni, *Physica*, 1967, **34**, 149.
- 27 L. Malikova, W. Krystek, F. H. Pollak, N. Dai, A. Cavus and M. C. Tamargo, *Phys. Rev. B*, 1996, **54**, 1819.
- 28 *CRC Handbook of Chemistry and Physics*, ed. D. R. Lide, CRC Press, Boca Raton, FL, 74th edn., 1994.